A Method of Moments Solution of a Cylindrical Cavity Placed Between Two Coaxial Transmission Lines

Mohammad A. Saed, *Member, IEEE*

Abstract—**This paper presents a method for analyzing a dielectric-filled cylindrical cavity separating two coaxial transmission lines. The method of analysis is based on the method of moments and the equivalence principle taking into account higher order modes excited at the junctions between the cavity and the two transmission lines. Expressions relating the cavity's scattering parameters to the structure dimensions and the dielectric parameters are derived and implemented numerically. Numerical simulation results as well as experimental results are presented. The method is also applied to the measurement of the dielectric parameters of certain dielectric materials.**

I. Introduction

In this paper, a cylindrical cavity filled completely with a dielectric material placed between two coaxial transmission lines, as shown in Fig. 1, is analyzed and tested. This structure, or a special case of it, can be used as the building block in the construction of coaxial filters [1]. Once the scattering parameters of this building block are derived, the overall characteristics of a filter consisting of several blocks can be obtained using matrix manipulation techniques [2]. Another application of the structure of Fig. 1 is the measurement of the complex permittivity of dielectric materials for the case where the dielectric material under test forms the dielectric filling the cavity.

Currently available techniques for measuring the complex permittivity of dielectric materials include the traditional cavity resonator techniques [3], [4] and the more recent wide-band time-domain techniques [5]–[8] and swept frequency techniques [9]–[12]. Many of the recent techniques require the insertion of a sample of the material under test into a coaxial air line, causing problems and air gap errors. The structure under consideration does not need insertion in a coaxial line; instead, the conductor walls of the cavity can be molded or deposited on the dielectric sample.

In this paper, a precise, full field analysis technique based on the method of moments [13] is used to derive expressions relating the scattering parameters of the cavity to its dimensions and the complex permittivity, ϵ^*, of the filling dielectric. These expressions are then implemented in two computer programs. One program calculates the scattering parameters, S_{11} and S_{21}, given ϵ^* and the cavity's dimensions ($S_{22} = S_{11}$ and $S_{12} = S_{21}$ from symmetry and reciprocity properties of the structure). The other program is an optimization program which calculates the dielectric's complex permittivity, ϵ^*, given any scattering parameter and the cavity's dimensions.

Manuscript received February 11, 1991; revised May 13, 1991.

The author is with the Electrical Engineering Department, State University of New York, College at New Paltz, New Paltz, NY 12561.

IEEE Log Number 9102326.

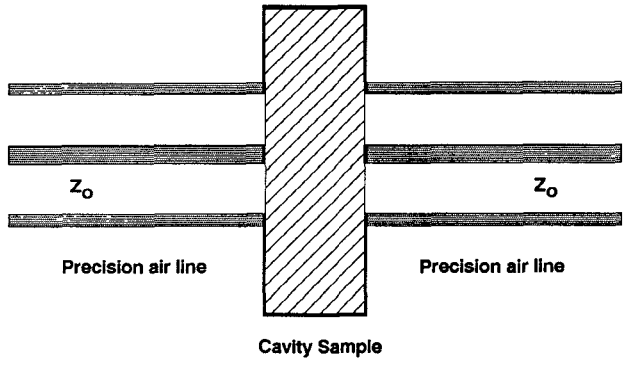

Fig. 1. Cylindrical cavity placed between two coaxial lines.

The derivation of the cavity's scattering parameters is presented in Section II. The optimization process to determine the complex permittivity given one of the scattering parameters and the cavity's dimensions is also described in Section II. Computer simulation and experimental results are presented in Section III. Finally, conclusions and discussions are presented in Section IV.

II. Derivation of the Scattering Parameters

The structure shown in Fig. 1 can be modeled as shown in Fig. 2 using the equivalence principle. Regions (a) and (c) are the regions of the transmission lines, and region (b) is the cavity region. The two apertures are replaced by perfect electric conductors on which the equivalent magnetic currents $-\vec{M}_1$ and $\vec{M}_2$ are imposed in the cavity region, region (b). To ensure the continuity of the electric field across the two apertures, the magnetic currents $\vec{M}_1$ and $-\vec{M}_2$ are placed on the apertures in the first and second transmission line regions (regions (a) and (c)), respectively, backed by perfect electric conductors, as shown in the figure. The magnetic current source, $\vec{M}_1$, equals the tangential component of the electric field over

0018-9480/91/1000-1712$01.00 ©1991 IEEE

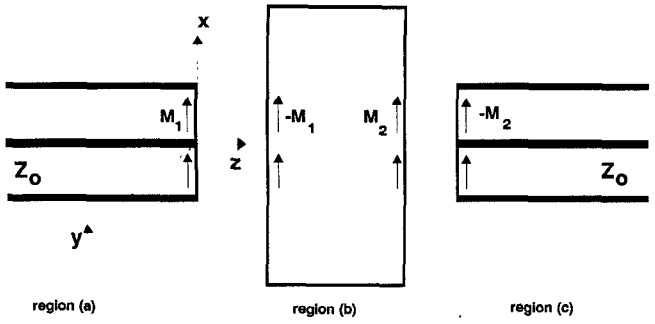

Fig. 2. Equivalent problem for structure in Fig. 1.

the first aperture; similarly, $\vec{M}_2$ equals the tangential component of the electric field over the second aperture. The unknown magnetic sources, $\vec{M}_1$ and $\vec{M}_2$, can be solved for by applying the remaining boundary condition, which is the continuity of the magnetic fields across the two apertures. This boundary condition yields the following two equations:

$$\left[2\vec{H}_t^i + \vec{H}_t^a(\vec{M}_1) = \vec{H}_{t1}^b(-\vec{M}_1) + \vec{H}_{t2}^b(\vec{M}_2)\right]_{\text{at } z=0} \quad (1)$$

$$\left[\vec{H}_{t1}^b(-\vec{M}_1) + \vec{H}_{t2}^b(\vec{M}_2) = \vec{H}_t^c(-\vec{M}_2)\right]_{\text{at } z=d} \quad (2)$$

where $\vec{H}_t^i$ is the tangential component of the incident magnetic field arising from the actual excitation source, $\vec{H}_t^a(\vec{M}_1)$ is the tangential magnetic field in region (a) arising from the magnetic source $\vec{M}_1$, $\vec{H}_{t1}^b(-\vec{M}_1)$ is the tangential magnetic field in region (b) caused by the magnetic source $-\vec{M}_1$, $\vec{H}_{t2}^b(\vec{M}_2)$ is the tangential magnetic field in region (b) arising from the magnetic source $\vec{M}_2$, $\vec{H}_t^c(-\vec{M}_2)$ is the tangential magnetic field in region (c) caused by the magnetic source $-\vec{M}_2$, and d is the cavity thickness. The incident magnetic field arising from the actual excitation source is assumed to be TEM mode. Expressions for the field components in (1) and (2) are obtained by solving the Helmholtz scalar equation and applying the proper boundary conditions [14].

In subsection A, the field components in the first transmission line region, region (a), are derived. Expressions for the field components in the cavity region, region (b), are derived in subsection B, and those in the second transmission line region are derived in subsection C. The application of the method of moments to obtain the solution is discussed in subsection D.

A. Region (a)

The structure under consideration is axially symmetric with no angular variation; therefore, the only higher order modes excited at the apertures are the TM_{0n} modes. The incident field arising from the actual excitation source is assumed to be TEM; consequently, the tangential component of the incident field at the first aperture, $\vec{H}_t^i|_{z=0}$, is given by

$$\vec{H}_t^i|_{z=0} = \frac{1}{\eta_0} e_0(\rho)\hat{a}_\phi \quad (3)$$

where $\eta_0 = \sqrt{\mu_0/\epsilon_0}$ is the intrinsic wave impedance (the transmission line is assumed to be an air line), and

$$e_0(\rho) = \frac{1}{\rho\sqrt{2\pi \ln(a/b)}} \quad (4)$$

with a and b the outer and inner radii of the transmission line, respectively. The transverse electric and magnetic field components arising from the magnetic current source M_1 can be written as

$$E_\rho^a(\vec{M}_1) = \sum_{n=0}^{\infty} A_n e_n(\rho) e^{\gamma_n z} \quad (5)$$

$$H_\phi^a(\vec{M}_1) = -\sum_{n=0}^{\infty} \frac{A_n}{\eta_n} e_n(\rho) e^{\gamma_n z} \quad (6)$$

where $e_0(\rho)$ is given in (4), A_n are unknown coefficients to be evaluated later, $\gamma_0 = j\omega\sqrt{\epsilon_0\mu_0}$, and, for $n \geq 1$,

$$e_n(\rho) = N_n[J_0(k_n b)Y_1(k_n\rho) - Y_0(k_n b)J_1(k_n\rho)], \quad n \geq 1 \quad (7)$$

$$\gamma_n = \sqrt{(k_n)^2 + (\gamma_0)^2}, \qquad n \geq 1 \quad (8)$$

$$\eta_n = \frac{\gamma_n}{j\omega\epsilon_0}, \qquad n \geq 1. \quad (9)$$

J_m and Y_m denote mth-order Bessel functions of the first and second kinds, respectively, and k_n is the solution of the following equation:

$$Y_0(k_n b)J_0(k_n a) = J_0(k_n b)Y_0(k_n a), \qquad n \geq 1. \quad (10)$$

N_n is a normalizing constant given by

$$N_n = \frac{1}{\sqrt{\pi(\alpha_n^2 - \beta_n^2)}}, \qquad n \geq 1 \quad (11)$$

where

$$\alpha_n = a[J_0(k_n b)Y_1(k_n a) - Y_0(k_n b)J_1(k_n a)] \quad (12)$$

$$\beta_n = b[J_0(k_n b)Y_1(k_n b) - Y_0(k_n b)J_1(k_n b)]. \quad (13)$$

The constants in (4) and (7) are computed such that $e_n(\rho)$ are orthonormal to simplify subsequent calculations; that is,

$$\int_0^{2\pi}\int_b^a e_n(\rho)e_m(\rho)\rho d\rho d\phi = \begin{cases} 1, & m = n \\ 0, & m \neq n. \end{cases} \quad (14)$$

The coefficients A_n in (5) and (6) can be obtained by applying the boundary condition

$$\vec{M}_1 = M_{1\phi}\hat{a}_\phi = \hat{a}_z \times \vec{E}^a|_{z=0} \quad (15)$$

where $\vec{E}^a$ is the electric field in region (a). Combining (5) and (15) and multiplying both sides of the resulting equation by $e_m(\rho)$, integrating over the first aperture, and using the orthonormality in (14), the following expression for A_n can be derived:

$$A_n = \int_0^{2\pi}\int_b^a M_{1\phi}e_n(\rho)\rho d\rho d\phi, \qquad n = 0,1,2,\cdots. \quad (16)$$

Hence, the transverse components of the magnetic fields in region (a) are given by (3), (6), and (16).

B. Region (b)

The transverse components of the electric and magnetic fields in region (b) can be written as

$$E_\rho^b = E_{1\rho}^b\left(-\vec{M}_1\right) + E_{2\rho}^b\left(\vec{M}_2\right) \tag{17}$$

$$H_\phi^b = H_{1\phi}^b\left(-\vec{M}_1\right) + H_{2\phi}^b\left(\vec{M}_2\right) \tag{18}$$

where

$$E_{1\rho}^b\left(-\vec{M}_1\right) = \sum_{n=1}^{\infty} B_n J_1(p_n\rho)\sin\zeta_n(z-d) \tag{19}$$

$$E_{2\rho}^b\left(\vec{M}_2\right) = \sum_{n=1}^{\infty} C_n J_1(p_n\rho)\sin\zeta_n z \tag{20}$$

$$H_{1\phi}^b\left(-\vec{M}_1\right) = j\omega\epsilon^* \sum_{n=1}^{\infty} \frac{B_n}{p_n} J_1(p_n\rho)\sin\zeta_n(z-d) \tag{21}$$

$$H_{2\phi}^b\left(\vec{M}_2\right) = j\omega\epsilon^* \sum_{n=1}^{\infty} \frac{C_n}{p_n} J_1(p_n\rho)\sin\zeta_n z \tag{22}$$

where $\zeta_n = [\omega^2\epsilon_r^*\epsilon_0\mu_0 - (p_n)^2]^{1/2}$ and p_n is obtained from the equation $J_0(p_nR) = 0$, R being the radius of the cavity. The coefficients B_n and C_n are evaluated by using the boundary conditions

$$-\vec{M}_1 = -M_{1\phi}\hat{a}_\phi = -\hat{a}_z \times \vec{E}^b|_{z=0} \tag{23}$$

$$\vec{M}_2 = M_{2\phi}\hat{a}_\phi = \hat{a}_z \times \vec{E}^b|_{z=d}. \tag{24}$$

Using (17), (18), (23), and (24) along with the orthogonality of Bessel functions, the following expressions for the coefficients B_n and C_n can be derived:

$$B_n = \frac{-2}{R^2 J_1^2(p_nR)\sin(p_nd)} \int_b^a M_{1\phi} J_1(p_n\rho)\rho\, d\rho, \qquad n = 1,2,\cdots \tag{25}$$

$$C_n = \frac{2}{R^2 J_1^2(p_nR)\sin(p_nd)} \int_b^a M_{2\phi} J_1(p_n\rho)\rho\, d\rho, \qquad n = 1,2,\cdots. \tag{26}$$

Hence, the transverse magnetic field components in region (b) are given by (21), (22), (25), and (26).

C. Region (c)

The electric and magnetic field components in region (c) are due to the magnetic current source $-\vec{M}_2$ only. The boundary condition that must be satisfied in this region is

$$-\vec{M}_2 = -\hat{a}_z \times \vec{E}^c|_{z=d}. \tag{27}$$

Following a procedure similar to that used in region (a), the following expression for the transverse component of the magnetic field is obtained:

$$H_\phi^c\left(-\vec{M}_2\right) = -\sum_{n=0}^{\infty} \frac{D_n}{\eta_n} e_n(\rho) e^{-\gamma_n z} \tag{28}$$

where η_n and $e_n(\rho)$ were defined in subsection A, and D_n is given by

$$D_n = \int_0^{2\pi}\int_b^a M_{2\phi} e_n(\rho)\rho\, d\rho\, d\phi, \qquad n = 0,1,2,\cdots. \tag{29}$$

D. Solution Using the Method of Moments

The method of moments [13] is used to solve (1) and (2) to obtain $\vec{M}_1$ and $\vec{M}_2$. Once the two magnetic current sources are obtained, the derivation of the scattering parameters is straightforward. The set of basis functions is taken to be the same as the set of weighting functions. The entire domain basis functions used are the modal functions of the coaxial lines, $e_n(\rho)$. The unknown magnetic current sources are expanded in terms of the basis functions as follows:

$$M_{1\phi} = \sum_{n=0}^{N} V_n e_n(\rho) \tag{30}$$

$$M_{2\phi} = \sum_{n=0}^{N} U_n e_n(\rho) \tag{31}$$

where N is the number of basis functions needed, and the coefficients V_n and U_n are to be determined. Substituting (30) and (31) into (1), multiplying both sides of the resulting equation by $e_m(\rho)$, and integrating over the first aperture using the transverse magnetic field expressions presented above in subsections A and B, after some lengthy manipulations, the following matrix equation can be derived:

$$\left[Y^a + Y_1^b\right]\vec{V} + Y_2^b\vec{U} = \vec{I}. \tag{32}$$

Similarly, (30), (31) and (2) can be combined to obtain the following matrix equation:

$$Y_2^b\vec{V} + \left[Y^a + Y_1^b\right]\vec{U} = 0 \tag{33}$$

where $\vec{V}$ and $\vec{U}$ are vectors of the unknown coefficients, V_n and U_n. The elements of the matrices in (32) and (33) are given by

$$Y_{mn}^a = \begin{cases} \dfrac{1}{\eta_{n-1}}, & m = n \\ 0, & m \neq n \end{cases} \tag{34}$$

$$Y_{1mn}^b = -j\omega\epsilon^* \sum_{n=1}^{\infty} \frac{F_{ni}F_{mi}}{\zeta_i \tan(\zeta_i d)} \tag{35}$$

$$Y_{2mn}^b = j\omega\epsilon^* \sum_{n=1}^{\infty} \frac{F_{ni}F_{mi}}{\zeta_i \sin(\zeta_i d)} \tag{36}$$

where

$$F_{ni} = \begin{cases} \dfrac{\sqrt{2}\left[J_0(p_ib) - J_0(p_ia)\right]}{p_iRJ_1(p_iR)\sqrt{\ln(b/a)}}, & n = 1 \\ \dfrac{2a\sqrt{\pi}N_n p_i\left[J_0(p_ia)\alpha_n - J_0(p_ib)\beta_n\right]}{RJ_1(p_iR)\left[(k_n)^2 - (p_i)^2\right]}, & n > 1. \end{cases} \tag{37}$$

N_n, α_n, and β_n were defined earlier in (11)–(13). The elements of the excitation vector, $\vec{I}$, are given by

$$I_n = \begin{cases} \dfrac{2}{\eta_0}, & n = 1 \\ 0, & m > n. \end{cases} \tag{38}$$

Equations (32) and (33) can be augmented into one matrix equation:

$$\begin{bmatrix} Y^a + Y_1^b & Y_2^b \\ Y_2^b & Y^a + Y_1^b \end{bmatrix} \begin{bmatrix} \vec{V} \\ \vec{U} \end{bmatrix} = \begin{bmatrix} \vec{I} \\ 0 \end{bmatrix}. \tag{39}$$

Equation (39) can be solved directly using a Gaussian elimination technique to obtain the vector of unknown coefficients. Once these coefficients, V_n and U_n, are obtained, the scattering parameters can be evaluated easily. Using the boundary conditions in (15) and (27) along with the expansions of (30) and (31) and the orthonormality property in (14), the following expressions for S_{11} and S_{21} are obtained:

$$S_{11} = V_1 - 1 \tag{40}$$

$$S_{21} = U_1 e^{\gamma_0 d}. \tag{41}$$

Also, $S_{22} = S_{11}$ and $S_{12} = S_{21}$ because of the symmetry and reciprocity properties of the structure under consideration.

A Fortran program implementing the above equations has been written. The number of modes taken into account in the three regions had to be determined to truncate the infinite series of (35) and (36). The criterion which gave fast convergence is the following:

$$N_a = N_c = \frac{a-b}{R} N_b \tag{42}$$

where N_a, N_b, and N_c are the numbers of modes in regions (a), (b), and (c), respectively. The program was used to perform several simulation experiments using different combinations of cavity dimensions and dielectric parameters. It was concluded that $N_a = 20$ was the proper choice to obtain satisfactory convergence for the combinations used.

In dielectric characterization applications, the complex permittivity, ϵ^*, is the unknown quantity. In this case, the elements of the matrices Y_1^b and Y_2^b are nonlinear functions of ϵ^*. Consequently, the solution is obtained iteratively given either the measured S_{11} or S_{21} parameter by minimizing a proper error function. If S_{11} is given, the following function is minimized subject to the matrix equation (39):

$$F_1(\epsilon^*) = |S_{11} - V_1 + 1|. \tag{43}$$

If S_{21} is to be used for the computation of ϵ^*, the solution is obtained by minimizing the following function subject to the matrix equation (39):

$$F_2(\epsilon^*) = |S_{21} - U_1 e^{\gamma_0 d}|. \tag{44}$$

The iterative procedure is as follows: first an initial guess of ϵ^* is made; then V_n's and U_n's are computed directly from (39) using Gaussian elimination. Only V_1 (or U_1) is needed to evaluate $F_1(\epsilon^*)$ (or $F_2(\epsilon^*)$). If the value of the error function being minimized is larger than a desired tolerance, ϵ^* is updated using Powell's hybrid method [15]. The new values of the V_n's and U_n's are then computed using (39) and again the error function is computed. This procedure is repeated until the desired tolerance is achieved. A computer program was written implementing the above optimization procedure in which the tolerance was chosen to be 10^{-10}.

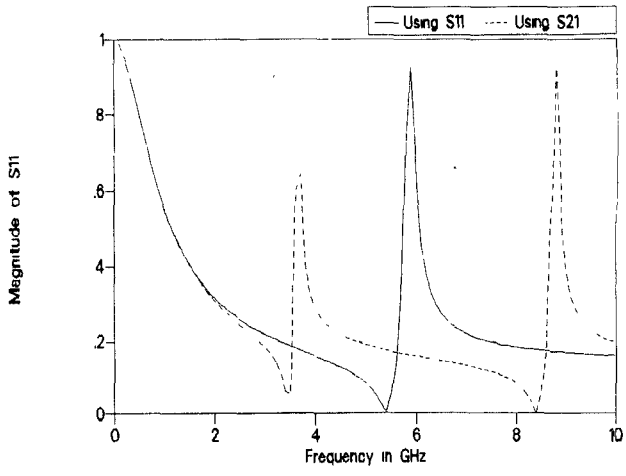

Fig. 3. Magnitude of S_{11} for two different sample radii ($d = 0.025$ cm, $\epsilon_r' = 5$, $\epsilon_r'' = 0$).

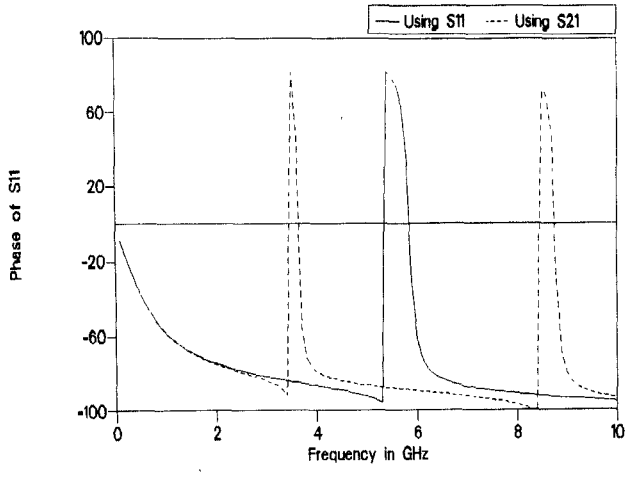

Fig. 4. Phase of S_{11} for two different sample radii ($d = 0.025$ cm, $\epsilon_r' = 5$, $\epsilon_r'' = 0$).

III. Numerical and Experimental Results

The scattering parameters of cavity samples with different dimensions were computed using one of the implemented computer programs. A sample result is shown in Figs. 3–6, where magnitudes and phases of S_{11} and S_{21} are shown for two sample radii: $R = 1$ cm and $R = 1.5$ cm. The other sample parameters were assumed as follows: thickness $d = 0.025$ cm, $\epsilon_r' = 5.0$, and $\epsilon_r'' = 0$. The resonance frequencies observed are due to the radial dimension; the resonance caused by the thickness occurs at a

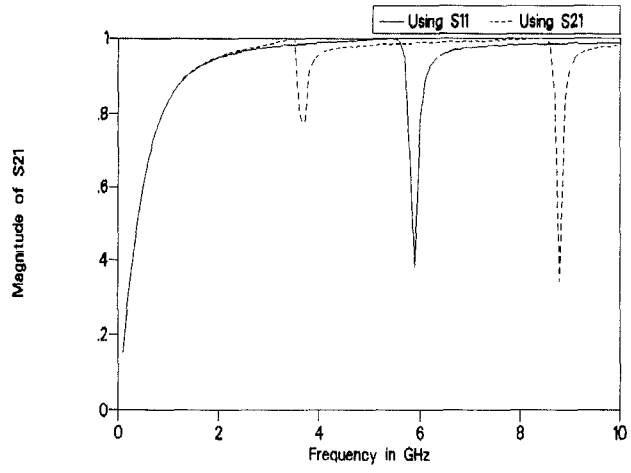

Fig. 5. Magnitude of S_{21} for two different sample radii ($d = 0.025$ cm, $\epsilon_r' = 5$, $\epsilon_r'' = 0$).

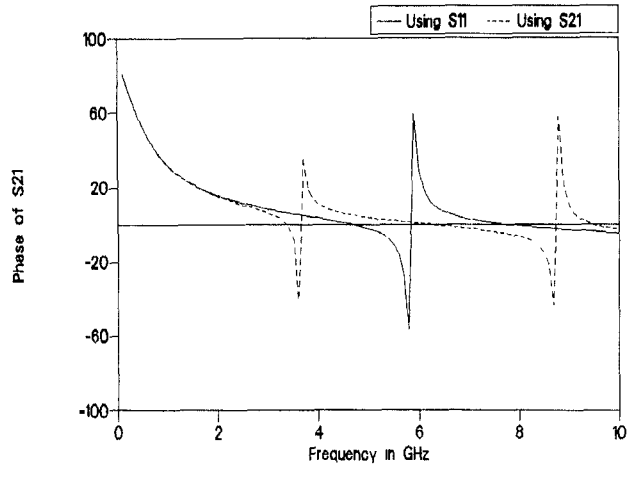

Fig. 6. Phase of S_{21} for two different sample radii ($d = 0.025$ cm, $\epsilon_r' = 5$, $\epsilon_r'' = 0$).

much higher frequency for the sample parameters chosen. Hence, the resonance frequency can be changed by changing the sample diameter or dielectric material. This was confirmed by testing several samples with different radii and thicknesses and it was observed that changing the thickness has no effect on the location of resonance.

The use of this structure in characterizing dielectric materials is demonstrated in Fig. 7. In this figure, the computed dielectric constant of a Teflon sample, which is known to have a dielectric constant of 2.1, is shown. The samples were constructed from a Teflon board with copper cladding on both sides. Circular disks were punched from the board; the copper was partially etched from both sides, leaving the proper apertures using a standard photolithographic etching process; and the sides were covered with silver paint to complete the cavity shape. The measurements were performed using the HP8510 vector network analyzer. The measured S_{11} and S_{21} were both used in the optimization program, and as observed in the figure, both yield results that are consistent with the known values. The dielectric loss results, however, were

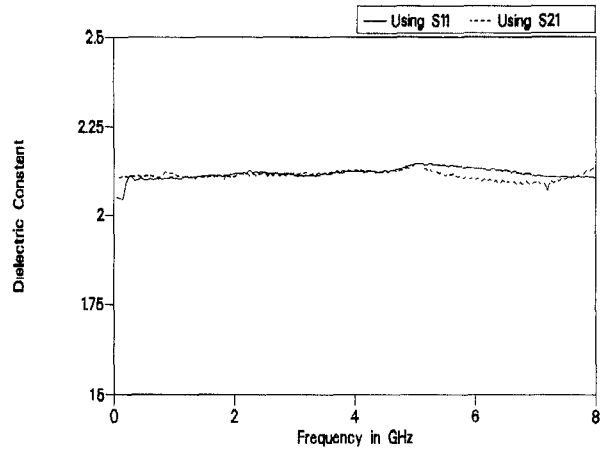

Fig. 7. Measured dielectric constant, ϵ_r', of a Teflon sample using S_{11} and S_{21} ($R = 0.75$ cm, $d = 0.0753$ cm).

not very accurate since Teflon has a very low loss. Low-loss dielectric materials require extreme precision in measuring the scattering parameters to obtain accurate estimates for the dielectric loss. Furthermore, the analysis may have to be revised to include losses in the conductor walls of the cavity.

IV. Conclusions

This paper presented the concept, analysis, and testing of a structure formed by placing a cavity between two coaxial transmission lines. The method of analysis is based on the method of moments taking into account higher order modes generated at the two apertures. The structure can be used as a building block in coaxial filters and it can be used in measuring the complex permittivity of dielectric materials. Theoretical and experimental results were presented confirming the validity of the analysis and computer implementation. The structure was successfully used to measure the dielectric constant of a known dielectric material. For low-loss dielectric materials, extreme precision in measuring the scattering parameters is needed to obtain reliable dielectric loss estimates. Furthermore, the analysis may have to be revised to include losses in the conductor walls of the cavity.

References

[1] G. L. Matthaei, L. Young, and E. M. Jones, *Microwave Filters, Impedance Matching Networks, and Coupling Structures*. New York: McGraw-Hill, 1964.

[2] D. Pozar, *Microwave Engineering*. Englewood Cliffs, NJ: Prentice Hall, 1990.

[3] R. J. Cook, "Microwave cavity methods," in *High Frequency Dielectric Measurement*, J. Chamberlain and G. W. Chantry, Eds. Guildford, U.K.: Science and Technology Press, 1973, pp. 12–27.

[4] D. C. Dube, M. T. Lanagan, J. H. Kim, and S. J. Jang, "Dielectric measurements on substrate materials at microwave frequencies using a cavity perturbation technique," *J. Appl. Phys.*, vol. 63, no. 7, pp. 2466–2468, Apr. 1988.

[5] M. J. V. Gemert, "High frequency time domain methods in dielectric spectroscopy," *Philips Res. Rep.*, vol. 28, pp. 530–572, Nov. 1973.

[6] R. H. Cole, "Evaluation of dielectric behavior by time domain spectroscopy—I: Dielectric response by real time analysis," *J. Phys. Chem.*, vol. 79, no. 14, pp. 1459–1469, 1975.
[7] R. H. Cole, "Time domain spectroscopy of dielectric materials," *IEEE Trans. Instrum. Meas.*, vol. IM-25, pp. 371–375, Dec. 1976.
[8] R. Chahine and T. Bose, "Comparative studies of various methods in time domain spectroscopy," *J. Chem. Phys.*, vol. 72, no. 2, pp. 808–815, 1980.
[9] W. B. Weir, "Automatic measurement of complex dielectric constant and permeability at microwave frequencies," *Proc. IEEE*, vol. 62, pp. 33–36, 1974.
[10] T. Athey, M. Stuchly, and S. Stuchly, "Measurement of radio frequency permittivity of biological tissues with an open ended coaxial line: Part I.," *IEEE Trans. Microwave Theory Tech.*, vol. MTT-30, pp. 82–86, Jan. 1982.
[11] M. Stuchly, T. Athey, G. Samaras, and G. Taylor, "Measurement of radio frequency permittivity of biological tissues with an open ended coaxial line: Part II—Experimental results," *IEEE Trans. Microwave Theory Tech.*, vol. MTT-30, pp. 87–92, Jan. 1982.
[12] L. P. Lighthart,"A fast computational technique for accurate permittivity determination using transmission line methods," *IEEE Trans. Microwave Theory Tech.*, vol. MTT-31, pp. 249–254, Mar. 1983.
[13] R. F. Harrington, *Field Computation by Moment Methods*. New York: Macmillan, 1968.
[14] R. F. Harrington, *Time Harmonic Electromagnetic Fields*. New York: McGraw-Hill, 1961.
[15] M. J. D. Powell, "A hybrid method for nonlinear equations," in *Numerical Methods for Nonlinear Algebraic Equations*, P. Rabinowitz, Ed. New York: Gordon Science Publishers, 1970, pp. 87–114.

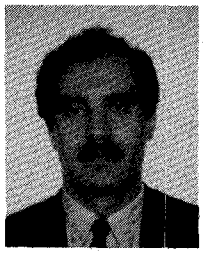

Mohammad A. Saed (M'89) was born in Tulkarm, Jordan, in 1962. He received the B.Sc. degree in electrical engineering from the Middle East Technical University, Ankara, Turkey, in 1983. He received the M.S. and Ph.D. degrees in electrical engineering from Virginia Polytechnic Institute and State University, Blacksburg, in 1984 and 1987, respectively.

He worked at Virginia Polytechnic as a postdoctoral research associate from December 1987 to August 1989. He then joined the Department of Electrical Engineering, State University of New York, College at New Paltz, where he is currently an Assistant Professor. His areas of interest include microwave measurements, microstrip antennas and arrays, and computational electromagnetics.